

Superconducting interfaces between insulating oxides

N. Reyren, Stefan Thiel, A. D. Caviglia, Lena F. Kourkoutis, German Hammerl, Christoph Richter, Christof W. Schneider, Thilo Kopp, A.-S. Ruetschi, D. Jaccard, M. Gabay, David A. Muller, Jean-Marc Triscone, Jochen Mannhart

Angaben zur Veröffentlichung / Publication details:

Reyren, N., Stefan Thiel, A. D. Caviglia, Lena F. Kourkoutis, German Hammerl, Christoph Richter, Christof W. Schneider, et al. 2007. "Superconducting interfaces between insulating oxides." *Science* 317 (5842): 1196–99.
<https://doi.org/10.1126/science.1146006>.

Superconducting Interfaces Between Insulating Oxides

N. Reyren,¹ S. Thiel,² A. D. Caviglia,¹ L. Fitting Kourkoutis,³ G. Hammerl,² C. Richter,² C. W. Schneider,² T. Kopp,² A.-S. Rüetschi,¹ D. Jaccard,¹ M. Gabay,⁴ D. A. Müller,³ J.-M. Triscone,¹ J. Mannhart^{2*}

At interfaces between complex oxides, electronic systems with unusual electronic properties can be generated. We report on superconductivity in the electron gas formed at the interface between two insulating dielectric perovskite oxides, LaAlO₃ and SrTiO₃. The behavior of the electron gas is that of a two-dimensional superconductor, confined to a thin sheet at the interface. The superconducting transition temperature of $\cong 200$ millikelvin provides a strict upper limit to the thickness of the superconducting layer of $\cong 10$ nanometers.

In pioneering work, it was demonstrated that a highly mobile electron system can be induced at the interface between LaAlO₃ and SrTiO₃ (1). The discovery of this electron gas at the interface between two insulators has generated an impressive amount of experimental and theoretical work (2–8), in part because the complex ionic structure and particular interactions found at such an interface are expected to promote novel

electronic phases that are not always stable as bulk phases (9–11). This result also generated an intense debate on the origin of the conducting layer, which could either be “extrinsic” and due to oxygen vacancies in the SrTiO₃ crystal or “intrinsic” and related to the polar nature of the LaAlO₃ structure. In the polar scenario, a potential develops as the LaAlO₃ layer thickness increases that may lead to an “electronic reconstruction” above some critical thickness (5). Another key issue concerns the ground state of such a system; at low temperatures, a charge-ordered interface with ferromagnetic spin alignment was predicted (4). Experimental evidence in favor of a ferromagnetic ground state was recently found (6). Yet, rather than ordering magnetically, the electron system may also condense into a superconducting state. It was proposed that in field effect transistor config-

urations, a superconducting, two-dimensional (2D) electron gas might be generated at the SrTiO₃ surface (12). It was also pointed out that the polarization of the SrTiO₃ layers may cause the electrons on SrTiO₃ surfaces to pair and form at high temperatures a superconducting condensate (13, 14). In this report, we explore the ground state of the LaAlO₃/SrTiO₃ interface and clarify whether it orders when the temperature approaches absolute zero. Our experiments provide evidence that the investigated electron gases condense into a superconducting phase. The characteristics of the transition are consistent with those of a 2D electron system undergoing a Berezinskii-Kosterlitz-Thouless (BKT) transition (15–17). In the oxygen vacancy scenario the observation of superconductivity provides a strict upper limit to the thickness of the superconducting sheet at the LaAlO₃/SrTiO₃ interface.

The samples were prepared by depositing LaAlO₃ layers with thicknesses of 2, 8, and 15 unit cells (uc) on TiO₂-terminated (001) surfaces of SrTiO₃ single crystals (5, 18). The films were grown by pulsed laser deposition at 770°C and 6×10^{-5} mbar O₂, then cooled to room temperature in 400 mbar of O₂, with a 1-hour oxidation step at 600°C. The fact that only heterostructures with a LaAlO₃ thickness greater than three uc conduct (5) was used to pattern the samples (19). Without exposing the LaAlO₃/SrTiO₃ interface to the environment, bridges with widths of 100 μm and lengths of 300 μm and 700 μm were structured for four-point measurements, as well as two-uc-thick LaAlO₃ layers for reference (18).

¹Département de Physique de la Matière Condensée, University of Geneva, 24 quai Ernest-Ansermet, 1211 Genève 4, Switzerland. ²Experimental Physics VI, Center for Electronic Correlations and Magnetism, Institute of Physics, University of Augsburg, D-86135 Augsburg, Germany. ³School of Applied and Engineering Physics, Cornell University, Ithaca, NY 14853, USA. ⁴Laboratoire de Physique des Solides, Bat 510, Université Paris-Sud 11, Centre d'Orsay, 91405 Orsay, Cedex, France.

*To whom correspondence should be addressed. E-mail: jochen.mannhart@physik.uni-augsburg.de

Transmission electron studies (18) were performed on reference samples grown under conditions identical to those described above. Cross-sectional cuts were prepared by mechanical polishing followed by low-energy, low-angle ion milling and investigated by scanning transmission electron microscopy (STEM) (18). Figure 1A shows a high-angle annular dark field (HAADF) STEM image of the sharp interface between a 15-uc-thick LaAlO₃ film and the SrTiO₃ substrate. The film is found to be coherent with the substrate with no obvious defects or dislocations at the interface, resulting in biaxial tensile strain of $\cong 3\%$, as measured from STEM images (18). The out-of-plane lattice

constant of the LaAlO₃ film is $\cong 3.78 \text{ \AA}$, which is close to the bulk value and suggests either a rather small Poisson ratio as previously reported (20) or out-of-plane relaxation in the thin film (21). To obtain an upper limit on the extent of electronic structure and compositional changes below the interface, electron energy-loss spectroscopy (EELS) in the STEM was used to probe the chemistry of the heterostructure at the atomic scale. Simultaneously recorded O-K and Ti-L_{2,3} edges close to and far away from the interface are shown in Fig. 1, B and C. By 1.5 nm away from the interface, the changes in the O-K edge are very slight, suggesting an upper limit to the oxygen vacancy concentration of 3%. At 6 nm

away from the interface, the changes in the O-K and Ti-L_{2,3} edges compared with bulk SrTiO₃ fall below the noise level ($<1\%$ oxygen vacancy concentration). The small changes of the Ti-L_{2,3} edges are consistent with a slight increase in Ti³⁺, either from oxygen deficiency (22) or a compensating interface charge (18).

Two samples were analyzed by transport measurements and found to be conducting (Fig. 2A), their 2-uc-thick control structures being insulating (resistance $R > 30 \text{ M}\Omega$) at all temperatures T ($32 \text{ mK} < T < 300 \text{ K}$). At $T \cong 4.2 \text{ K}$, the Hall carrier densities of the 8-uc and 15-uc samples equal $\cong 4 \times 10^{13}/\text{cm}^2$ and $\cong 1.5 \times 10^{13}/\text{cm}^2$, and the mobilities $\cong 350 \text{ cm}^2/\text{Vs}$ and $\cong 1000 \text{ cm}^2/\text{Vs}$, respectively. Whether the differences in the sample properties present an intrinsic effect that is caused by the variation of the LaAlO₃ thickness remains to be explored. The Hall response is only weakly temperature dependent [$\text{Hall resistance } R_H(300 \text{ K})/R_H(4.2 \text{ K}) \cong 0.8$ and 0.95 for the 8-uc and 15-uc samples, respectively]. Magnetic fields up to $\mu_0 H = 8 \text{ T}$ were applied to the 8-uc-thick sample, revealing a positive magnetoresistance. The samples investigated here do not show a hysteretic magnetoresistance. No minimum is found in the $R(T)$ characteristics of the 8-uc sample, such as was reported recently for LaAlO₃/SrTiO₃ samples fabricated under different conditions (6). For the 15-uc sample, a shallow minimum in the $R(T)$ curve was observed at 4 K.

At $\cong 200 \text{ mK}$ and $\cong 100 \text{ mK}$, respectively, the 8-uc and 15-uc samples undergo a transition into a state for which no resistance could be measured (Fig. 2A). The widths of the transitions (20% to 80%) of the 8-uc and 15-uc samples are $\cong 16 \text{ mK}$ and $\cong 51 \text{ mK}$, respectively. The resistance drops by more than three orders of magnitude to below the noise limit of the measurement (18). Application of a magnetic field $\mu_0 H = 180 \text{ mT}$ perpendicular to the interface completely suppresses this zero-resistance state (Fig. 2B). Figure 3A displays the voltage versus current (V - I) characteristics of a bridge in the 8-uc sample, measured using a dc technique. At low temperatures, the V - I characteristics show a well-defined critical current I_c . The occurrence of the zero-resistance state and the characteristic $R(T, H)$ and $V(I, H)$ dependencies provide clear evidence for superconductivity.

The $T_c(H)$ dependence, where T_c is defined as $R(T_c) = 0.5 \times R(1 \text{ K})$, provides a measure for the upper critical field $H_{c2}(T)$. The $H_{c2}(T)$ curve is shown in Fig. 2C; $H_{c2}(0 \text{ K}) \cong 65 \text{ mT}$ and $\cong 30 \text{ mT}$ for the 8-uc and 15-uc samples, corresponding to coherence lengths $\xi(0 \text{ K}) \cong 70 \text{ nm}$ and $\cong 105 \text{ nm}$, respectively. Figure 3B shows the temperature dependence of the critical currents per unit width. The maximal values of I_c are $98 \mu\text{A}/\text{cm}$ and $5.6 \mu\text{A}/\text{cm}$ for the 8-uc and 15-uc samples, respectively. A steplike structure in the $V(I)$ curves displayed by the 15-uc sample (not shown) indicates that the low I_c of this sample is caused by inhomogeneities. Just below I_c , the

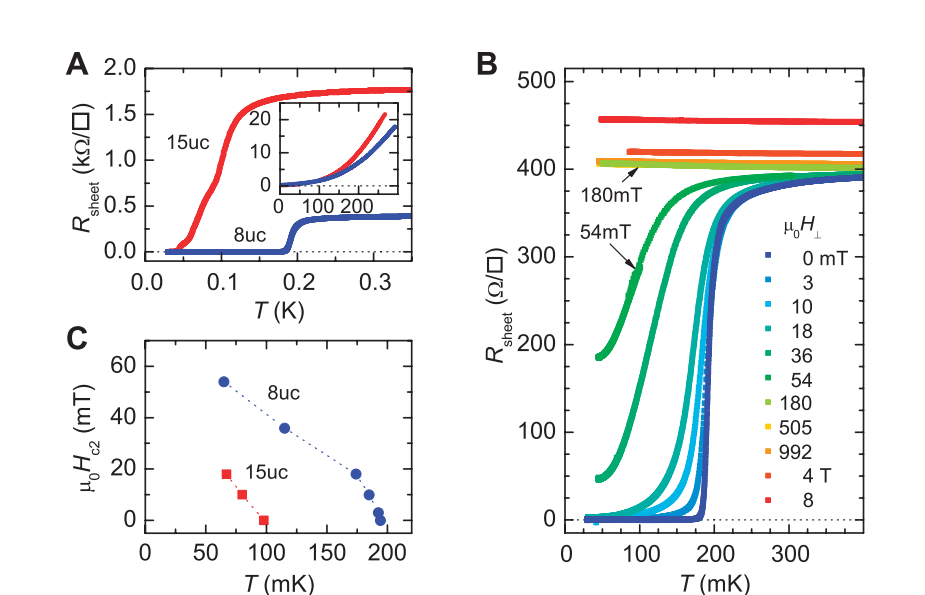
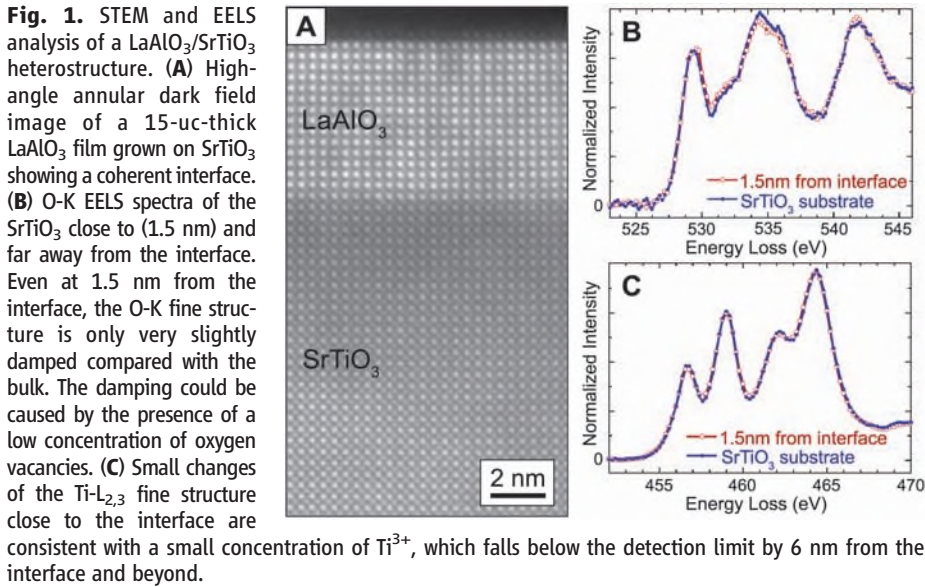


Fig. 2. Transport measurements on LaAlO₃/SrTiO₃ heterostructures. (A) Dependence of the sheet resistance on T of the 8-uc and 15-uc samples (measured with a 100-nA bias current). (Inset) Sheet resistance versus temperature measured between 4 K and 300 K. (B) Sheet resistance of the 8-uc sample plotted as a function of T for magnetic fields applied perpendicular to the interface. (C) Temperature dependence of the upper critical field H_{c2} of the two samples.

samples develop a small voltage drop which is proportional to the current and increases with temperature. As Fig. 4A shows for the 8-uc-thick sample, at 30 mK the associated resistance is at least four orders of magnitude smaller than the normal state resistance. With T increasing from 30 mK to 180 mK, the resistance grows exponentially from $\approx 0.1 \Omega$ to 10Ω . Between 180 mK and T_c , the step at I_c disappears and power-law type $V(I)$ curves are measured.

Is the bulk of the SrTiO₃ superconducting or is it only a thin sheet at the interface layer?

How thick is the superconducting layer? If the heterostructures were 2D superconductors, the transition into the superconducting state would be a BKT transition, characterized by a transition temperature T_{BKT} at which vortex-antivortex pairs unbind (23). A simple estimate of T_{BKT} , assuming that the sheet superconducting carrier density equals $4 \times 10^{13}/\text{cm}^2$, would suggest that in the samples, the BKT and mean field temperatures almost coincide. However, in case of large vortex fugacity, a high density of vortex-antivortex pairs is thermally generated and an ionic-like

vortex-antivortex crystal is formed (24). For such a system, the melting of this lattice represents the BKT transition, which then occurs at lower temperatures. At the BKT transition, the current-induced Lorentz force causes dislocation-antidislocation pairs to unbind, resulting in a $V \propto I^a$ behavior, with $a(T_{\text{BKT}}) = 3$.

The samples indeed show clear signatures of the BKT behavior, such as a $V \propto I^a$ power-law dependence (Fig. 4A). As revealed by Fig. 4B, at $T = 188$ mK, the exponent a approaches 3; this temperature is therefore identified as T_{BKT} . The $V(I, T)$ characteristics (Fig. 4A) are very similar to the results of simulations treating finite-size 2D systems (25). The ohmic regime observed below T_{BKT} at small currents is expected for finite size samples and agrees quantitatively with an analysis (18) based on (24).

In addition, the $R(T)$ characteristics are consistent with a BKT transition, for which, close to T_{BKT} , a $R = R_0 \exp(-bt^{-1/2})$ dependence is expected (26). Here, R_0 and b are material parameters and $t = T/T_{\text{BKT}} - 1$. As shown by Fig. 4C, the measured $R(T)$ dependence is consistent with this behavior and yields $T_{\text{BKT}} \approx 190$ mK, in agreement with the result of the a -exponent analysis. The superconducting transition of the samples is therefore consistent with that of a 2D superconducting film. Hence, the superconducting layer is thinner than $\xi \approx 70$ nm.

Analysis of the superconducting transition temperature provides an independent bound on the layer thickness. If the superconductivity were due to oxygen defects in SrTiO_{3-x}, a carrier density of $\geq 3 \times 10^{19}/\text{cm}^3$ would be required for a T_c of 200 mK (27). The measured sheet carrier densities thus give an upper limit for the thickness of the superconducting sheet of ≈ 15 nm. Considering that the carrier concentration of the SrTiO_{3-x} layer cannot be constant but has to conform to a profile following Poisson's equation as treated with consideration to the field-dependent SrTiO₃ susceptibility (28), one can set an upper limit for the thickness of the superconducting sheet of ≈ 10 nm, a value much smaller than that suggested in (7, 8) for the thickness of the conducting layer in reduced LaAlO₃/SrTiO₃ heterostructures. The carrier density profile at interfaces in oxygen-deficient SrTiO_{3-x} has also been calculated in (8). As a result of this model, a sheet carrier density $> 5 \times 10^{14}/\text{cm}^2$ is needed to provide a carrier concentration of $3 \times 10^{19}/\text{cm}^3$. Because the sheet carrier densities of our samples equal only 1.5 to $4 \times 10^{13}/\text{cm}^2$, according to this model the superconductivity of the LaAlO₃/SrTiO₃ interface cannot be caused by doped SrTiO_{3-x} alone.

The experiments presented here do not allow us to determine whether the observed superconductivity is due to a thin doped SrTiO₃ sheet or a novel phenomenon occurring at this artificial interface. Although the T_c of the heterostructures falls in the transition range of oxygen-deficient SrTiO_{3-x}, the transport properties of the samples differ to some extent from the ones of doped

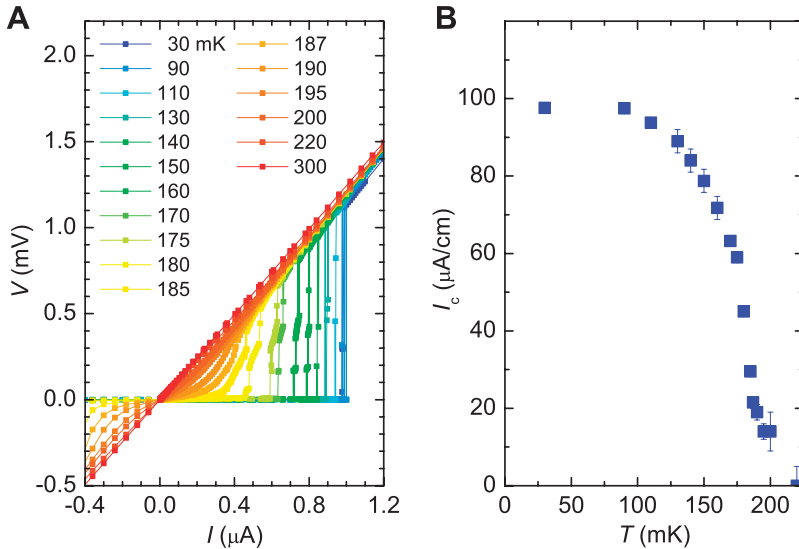


Fig. 3. $V(I)$ measurements of the 8-uc LaAlO₃/SrTiO₃ heterostructure. (A) Temperature-dependent voltage-current characteristics of a $100 \times 300 \mu\text{m}^2$ bridge. (B) Measured temperature dependence of the linear critical current density, as obtained from (A).

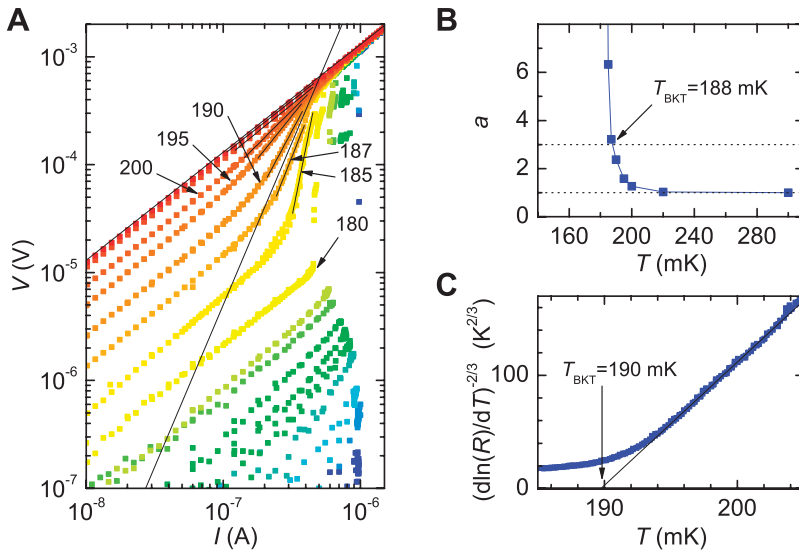


Fig. 4. Low-temperature transport properties of the 8-uc LaAlO₃/SrTiO₃ heterostructure. (A) $V(I)$ curves on a logarithmic scale. The color code is the same as that in Fig. 3A. The numbers provide the value of T , measured in mK, at which the curves were taken. The short black lines are fits of the data in the transition. The two long black lines correspond to $V = RI$ and $V \sim I^3$ dependencies and show that $187 \text{ mK} < T_{\text{BKT}} < 190 \text{ mK}$. (B) Temperature dependence of the power-law exponent a , as deduced from the fits shown in (A). (C) $R(T)$ dependence of the 8-uc sample ($I = 100 \text{ nA}$), plotted on a $[d\ln(R)/dT]^{-2/3}$ scale. The solid line is the behavior expected for a BKT transition with $T_{\text{BKT}} = 190 \text{ mK}$.

SrTiO₃. Whereas in oxygen-deficient SrTiO_{3-x} and Nb-doped SrTiO₃ films the Hall constant increases markedly below 100 K (29), it is less temperature dependent in LaAlO₃/SrTiO₃ heterostructures. In addition, the upper critical field of the heterostructures is an order of magnitude smaller than that of Nb-SrTiO₃ with the same T_c . Finally, our observation of both superconducting and insulating behavior on the same sample, depending on the precise LaAlO₃ layer thickness, is very hard to reconcile with a pure oxygen vacancy scenario.

References and Notes

1. A. Ohtomo, H. Y. Hwang, *Nature* **427**, 423 (2004).
2. N. Nakagawa, H. Y. Hwang, D. A. Muller, *Nat. Mater.* **5**, 204 (2006).
3. M. Huijben *et al.*, *Nat. Mater.* **5**, 556 (2006).
4. R. Pentcheva, W. E. Pickett, *Phys. Rev. B* **74**, 035112 (2006).
5. S. Thiel, G. Hammerl, A. Schmehl, C. W. Schneider, J. Mannhart, *Science* **313**, 1942 (2006).
6. A. Brinkman *et al.*, *Nat. Mater.* **6**, 493 (2007).
7. G. Herranz *et al.*, *Phys. Rev. Lett.* **98**, 216803 (2007).
8. W. Siemons *et al.*, *Phys. Rev. Lett.* **98**, 196802 (2007).
9. S. Altieri, L. H. Tjeng, G. A. Sawatzky, *Thin Solid Films* **9**, 400 (2001).
10. S. Okamoto, J. Millis, *Nature* **428**, 630 (2004).
11. J. Mannhart, in *Thin Films and Heterostructures for Oxide Electronics*, S. Ogale, Ed. (Springer, New York, 2005), pp. 251–278.
12. M. Gurvitch, H. L. Stormer, R. C. Dynes, J. M. Graybeal, D. C. Jacobson, in *Proceedings of the MRS*, J. Bevk, A. I. Braginski, Eds. (Materials Research Society, Warrendale, PA, 1986), pp. 47–49.
13. V. Koerting, Q. Yuan, P. J. Hirschfeld, T. Kopp, J. Mannhart, *Phys. Rev. B* **71**, 104510 (2005).
14. N. Pavlenko, T. Kopp, *Phys. Rev. B* **72**, 174516 (2005).
15. V. L. Berezinskii, *Zh. Eksp. Teor. Fiz.* **61**, 1144 (1971).
16. V. L. Berezinskii, *Sov. Phys. JETP* **34**, 610 (1972).
17. J. M. Kosterlitz, D. J. Thouless, *J. Phys. C* **5**, L124 (1972).
18. Materials and methods are available as supporting material on Science Online.
19. C. W. Schneider, S. Thiel, G. Hammerl, C. Richter, J. Mannhart, *Appl. Phys. Lett.* **89**, 122101 (2006).
20. J.-L. Maurice *et al.*, *Phys. Stat. Sol. (A)* **203**, 2209 (2006).
21. M. M. J. Treacy, J. M. Gibson, *J. Vac. Sci. Tech. B* **4**, 1458 (1986).
22. D. A. Muller, N. Nakagawa, A. Ohtomo, J. L. Grazul, H. Y. Hwang, *Nature* **430**, 657 (2004).
23. M. R. Beasley, J. E. Mooij, T. P. Orlando, *Phys. Rev. Lett.* **42**, 1165 (1979).
24. M. Gabay, A. Kapitulnik, *Phys. Rev. Lett.* **71**, 2138 (1993).
25. K. Medvedeva, B. J. Kim, P. Minnhagen, *Phys. Rev. B* **62**, 14531 (2000).
26. B. I. Halperin, D. R. Nelson, *J. Low Temp.* **36**, 599 (1979).
27. C. S. Koonce, M. L. Cohen, J. F. Schooley, W. R. Hosler, E. R. Pfeiffer, *Phys. Rev.* **163**, 380 (1967).
28. K. Ueno, thesis, University of Tokyo (2003).
29. K. S. Takahashi *et al.*, *Nature* **441**, 195 (2006).
30. The authors acknowledge fruitful discussions and interactions with D. Matthey and D. G. Schlom. This work was supported by the Swiss National Science Foundation through the National Centre of Competence in Research “Materials with Novel Electronic Properties” and the Swiss National Science Foundation Division II, by the Bundesministerium für Bildung und Forschung through Elektronische Korrelationen und Magnetismus (13N6918), by the Deutsche Forschungsgemeinschaft through the Sonderforschungsbereich 484, by the European Union through Nanoxide, by the European Science Foundation through the “Thin Films for Novel Oxide Devices” program, and by the U.S. National Science Foundation.

Supporting Online Material

www.sciencemag.org/cgi/content/full/1146006/DC1

Materials and Methods

References